Ionization in atmospheric-pressure Helium plasma jets

Pedro Arsénio Nunes Aleixo Viegas
pedro.a.viegas@ist.utl.pt

Extended abstract of the thesis to obtain the Master of Science Degree in Engineering Physics

Instituto de Plasmas e Fusão Nuclear, Instituto Superior Técnico,
Universidade de Lisboa, Av. Rovisco Pais nr. 1, 1049-001 Lisboa, Portugal

(Dated: June 2015)

The optimization of medical applications of helium-based plasma jets depends on our knowledge of the kinetics of electrons and heavy-species in the plasma. This work studies different elementary processes controlling the global discharge behavior and the kinetics of the main charged and neutral species in helium / nitrogen / oxygen plasmas. Numerical simulations of the electron-impact reactions in Helium-based plasmas are performed using the IST-LoKI (LisbOn KInetics) computational tool. The influence of He metastable states and consequent superelastic and stepwise ionization collisions are documented, as well as the influence of the admixture of air gases with different collision cross sections and ionization thresholds. For a relative density of the molecular gas of only 0.1%, the calculated ionization rate coefficient is shown to be higher than in pure He. The addition of the electronegative gas O_2 is shown to have an effect in the effective ionization coefficient of the mixture. Particle balance equations have been solved for a pure helium plasma at atmospheric-pressure at steady-state for different electron densities using IST-LoKI. This study has allowed to identify species and reactions that should be included or discarded in a reduced kinetic scheme, with emphasis on the charge production and loss mechanisms in the plasma. The temporal evolution of species and reaction rates has been calculated for a reduced He-N_2 kinetic scheme, considering the local application of a transitory electric field with 50Td maximum amplitude, using the tool ZDPlasKin. The key role of the N_2 admixture in He and of various elementary processes, especially Penning reactions, on the ionization degree of the plasma is pointed out.

Keywords: Plasma jets, Helium, Electron kinetics, Chemical kinetics, Ionization, Medical applications of plasmas

I. INTRODUCTION

In the last few years, helium plasmas at atmospheric-pressure and room-temperature have received considerable interest due to their potential for biomedical applications. They can lead to the production of energetic species when interacting with the N_2 and O_2 in open air or when a molecular gas is added to enhance the generation of reactive radicals and ions, through collisions between electrons and neutrals. In particular, the propagation of atmospheric-pressure helium-mixture microplasma jets in long capillary tubes is being studied for the development of medical devices [1, 2]. So far, most experiments have been dedicated to the study of the plasma plume propagating in air. But for endoscopic treatments with jets, it is also important to better understand and optimize the propagation of discharges in long dielectric tubes as catheters. Recently, different experiments have been carried out to study the dynamics of these plasmas in tubes [3, 4].

In this context, mixtures involving small quantities of nitrogen, oxygen or synthesized air (80%N_2-20%O_2) have acquired great importance. The experimental results available on this subject do not allow a deep understanding of the phenomena involved. Modeling of plasma propagation can be used for comparison with experiments and to gain physical insight into various phenomena. The optimization of applications requires identifying and understanding the elementary processes controlling the global behavior of the discharge and the kinetics of the main charged and neutral species in helium / nitrogen / oxygen plasmas. There is also the need to understand the development of plasma jets and how charge production and destruction in the channel influences the jet propagation.

In this context, the development of state-of-the-art collisional radiative models (CRMs) is of great interest. CRMs are simulation tools for the kinetic description of discharge plasmas, which aim at obtaining the populations of the species within the plasma as well as their creation and loss rates, relating them to the discharge maintenance characteristics. The results of CRMs can be subsequently used to 'reduce' complex kinetic schemes and allow their utilization in heavier codes, by revealing the dominant factors governing the different parameters and by identifying the most important populations and rates for the system under study. The definition of a reduced scheme should provide a consistent analysis of the helium-based plasma ignition and of its propagation in dielectric tubes.

II. MODELS AND RESULTS

This master thesis is the result of work developed in both the EM2C (Energétique Moléculaire et Macroscopique, Combustion) laboratory at École Centrale Paris and the Gas Discharges and Gaseous Electronics (GEDG) group of IPFN (Instituto de Plasmas e Fusão Nuclear) at Instituto Superior Técnico - Universidade de Lisboa. Therefore, it benefits from the competences of both laboratories and from working with different teams of researchers. This context provides a unique background of research subjects, models and working tools for the development of the thesis.

In this work, the tool IST-LoKI (LisbOn KInetics) developed at the GEDG group is adapted and used to study the plasma kinetics in the aforementioned conditions. IST-LoKI is a self-consistent numerical code that solves the two-term electron Boltzmann equation (EBE) together with a system of balance equations describing the creation and loss processes of the dominant species, taking into account the given elementary processes.

The input parameters to the model are the electron density, the gas temperature, the pressure, the oscillation frequency of the electric field and the tube radius for diffusion rate purposes. The tool IST-LoKI allows to easily change the gas mixture, the species, rate coefficients and reaction rates to calculate and obtain the corresponding densities and plasma parameters. However, at the starting point of this work, the tool was prepared to solve systems of Argon, Nitrogen and Oxygen mixtures. In order to use IST-LoKI for different gas mixtures, the developer must first prepare the code for new electron-neutral cross section data, new species and new reactions and test the coherence of the results, by comparing them with results from other numerical tools and from experiments.

A. Electron kinetics

CRMs require knowledge about collisional–radiative data (cross sections for interactions with electrons, collision rate coefficients and radiative decay frequencies for interactions between heavy species) and transport parameters, to solve the rate balance equations of the different species in the plasma, coupled with the electron Boltzmann equation (EBE). The EBE is the equation that describes electrons in the plasma and that allows to obtain the non-equilibrium electron energy distribution function (EEDF) $f_e(v_e)$ [5]:

$$\frac{\partial f_e(\vec{r},\vec{v_e},t)}{\partial t} + \vec{v_e}.\vec{\nabla}_r f_e(\vec{r},\vec{v_e},t) - \frac{e}{m_e}\vec{E}(\vec{r},t).\vec{\nabla}_v f_e(\vec{r},\vec{v_e},t) = \\ = \left(\frac{\partial f_e}{\partial t}\right)_{coll}(\vec{r},\vec{v_e},t) \quad (1)$$

The solution to the Boltzmann equation for a specific gas or gas mixture yields the EEDF, allowing to determine the electron mean kinetic energy (associated with T_e) and all the electron transport parameters and rate coefficients, as function of the reduced electric field E/N, the quantity that links these input parameters to the discharge equations. For the particular case of the electron-impact reaction rate coefficients k_s for collisions with cross section $\sigma(v_e)$,

$$k_s(E/N) = \langle \sigma(v_e) v_e \rangle = \int \sigma(v_e) v_e f_e(E/N) 4\pi v_e^2 dv_e \quad (2)$$

These coefficients are essential to calculate the rates of creation and destruction of the species involved in electron-impact reactions, that play a role in plasma kinetics. The electric field accelerates the electrons, which acquire enough energy to undergo not only elastic but specially inelastic collisions with the gas neutral species, of which electron-impact ionization reactions are essential to firstly create the plasma. Therefore, solving the EBE allows us to witness the influence of the gas mixture and the applied field on the EEDF, considering the particular chracteristics of each gas. The EEDF provides information necessary to determine the concentrations of the species created by electron-impact and to monitor their evolution with changes in the gas mixture.

The EBE solver module of IST-LoKI has E/N, the gas mixture and the corresponding collisional cross sections as input data. The electric field is stationary and the system is solved for a steady-state case. Electron-electron collisions are not taken into account, due to the low ionization degrees involved and the EBE is written neglecting the production of secondary electrons born in ionization events and the loss of electrons due to diffusion and recombination, as these mechanisms are expected to have only second-order effects on the EEDF, at atmospheric-pressure.

The present study focuses first on the EEDF of helium-containing plasmas, calculated for several values of the reduced electric field (E/N). In particular, the effects of small admixtures of N_2, O_2 and synthesized air, and the influence of He metastables (He(2^3S) and He(2^1S)), involved in stepwise ionization and in superelastic collisions, are investigated.

With that intent, three cross section sets were created to serve as input to the numerical solver, using the cross section data from *Santos et al. (2014)* [6]. One of these sets includes cross sections for the elastic, electronic excitation and ionization collisions between electrons and ground-state He (He(1^1S), statistical weight $g = 1$). The other two sets account for the elastic, electronic excitation and ionization collisions between electrons and metastable excited states He(2^3S) ($g = 3$) and He(2^1S) ($g = 1$). The consistency of the EBE resolution is verified by the electron energy conservation. In fact, the EBE (1) embeds the elec-

tron mean-power balance given by [6]:

$$P_E + P_{sup} = P_{el} + P_{exc} + P_{ion} \tag{3}$$

The terms on the left-hand-side of eq. (3) represent, in order, the mean power absorbed from the field per electron P_E and the mean power gained in superelastic collisions P_{sup}, whereas the terms on the right-hand-side represent the mean power lost in elastic collisions with ground-state and excited-state atoms P_{el}, in excitations P_{exc} and in ionizations P_{ion}, respectively. Energy conservation requires the gain and loss terms to compensate each other. Detailed expressions for the power terms can be found in [7].

1. *Solution for Helium plasmas*

The first step required in the task of studying Helium is its inclusion in the program database and the validation of the corresponding results. When we consider pure He, the EBE is solved for the e^- + He(1^1S) collision cross sections from [6] only and there is no effect of superelastic collisions. Excitation of ground-state Helium by electron collision has a first energy threshold at 19.82 eV and the ionization of this state has a threshold of 24.59 eV.

The power gained by electrons from the electric field increases with E/N. The power lost by electrons in elastic and inelastic collisions also increases with E/N, since a higher amount of electrons have internal energies for higher cross sections. The accuracy of the numerical calculations is checked by comparing the gained and lost powers. The balance of eq. 3 is verified perfectly for $E/N < 200$ Td.

The reduced Townsend ionization coefficient $\alpha/N = K_{ion}/v_{de}$, calculated for E/N between 0.01 Td and 300 Td and for the case of pure ground-state He, was compared to that obtained from the on-line Boltzmann solver Bolsig+ [5], using the cross section databases of IST-Lisbon and three different models: no energy sharing, pulsed Townsend (PT) model and steady-state Townsend (SST) model. They were also compared to the results published in *Santos et al. (2014)* [6], that used a different code and additional cross sections, and to experimental values available on the LXCat on-line platform [8]. These comparisons allow us to evaluate the validity of the EEDF calculation in IST-LoKI and are presented in figure 1. As stated in [6], there is a good agreement of the calculated parameters with experiments for $E/N \leq 100$ Td. We can notice that the LoKI results agree with those of [6], which means that the inclusion of further excitation cross sections towards levels $n^{2S+1}l, 4 \leq n \leq 7$ would not provoke a significant change in the calculated EEDF.

Some He atomic metastable states have long lifetimes. They will not disappear quickly by radiative decay and, on the contrary, will continuously collide with electrons and

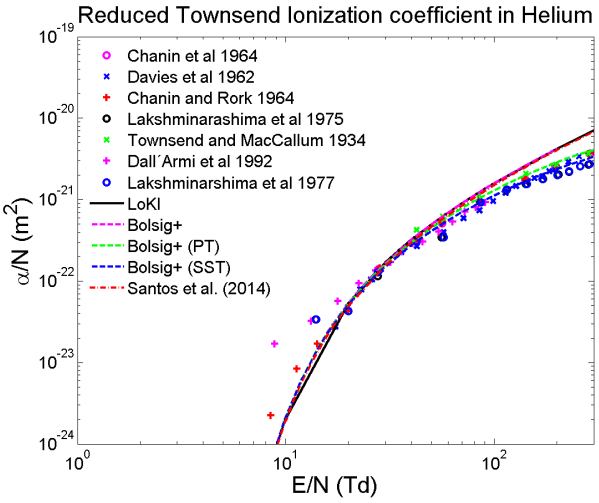

Figure 1. Reduced ionization Townsend coefficient for pure He(1^1S) as f(E/N) from several models and experiments.

influence the EEDF. Among the metastable states, the ones with principal quantum number n=2, He(2^3S) and He(2^1S), are the ones with more relevant densities. According to [6], their relative densities with respect to the ground-state densities are expected to be between 10^{-9} and 10^{-6}. When a relative density is set for the excited states He(2^3S) (statistical weight $g = 3$) and He(2^1S) ($g = 1$), electrons also collide with these states and the corresponding collision cross sections will take part in the calculation of the EEDF. These metastable states are introduced as a different species, meaning that the gas is a mixture of ground-state He(1^1S) and excited states He(2^3S) and He(2^1S). The new collision cross sections include inelastic excitation and ionization collisions that lead the excited states to upper levels and superelastic collisions, bringing the metastable states back to lower levels. The superelastic electron cross sections are calculated using the Klein-Rosseland relation:

$$\sigma_j^i(u) = \frac{\sigma_i^j(u + \Delta u_i^j)(u + \Delta u_i^j)}{u} \frac{g_i}{g_j} \tag{4}$$

where u is the electron energy, $\Delta u_i^j \equiv u_j - u_i > 0$ is the energy threshold for the transition from level i to level j and g_i and g_j are the statistical weights of the lower and upper levels, respectively.

The influence of He metastables on the EEDF is noted mostly at low reduced electric fields. Figure 2 shows the case for 1 Td, when the relative density of He(2^3S) is increased from 0 to 10^{-4}. It is seen that electron-He(2^3S) superelastic collisions turn the EEDF more energetic, creating a plateau up to the He(2^3S) threshold at 19.82 eV, corresponding to the energy gained by one electron in a superelastic collision. This plateau effect had already been reported in [5, 9]. The addition of the inelastic processes

also plays a role on the EEDF shape. We notice on figure 2 that the EEDF is high at very low energies (0-1 eV) and that there is a deep fall until $\sim$ 3 eV, in the region where the new inelastic cross sections matter the most. After the plateau region, there is once again a drop of f_e due to inelastic collisions with both He(1^1S) and He(2^3S). The higher the metastable densities, the deeper the falls of f_e. The effect of superelastic and inelastic collisions is the same for the cases with He(2^1S) densities instead of He(2^3S) and the case with both metastable states with equal relative densities. In summary, the addition of these relative densities provides more energetic EEDFs, due to the effect of superelastic collisions.

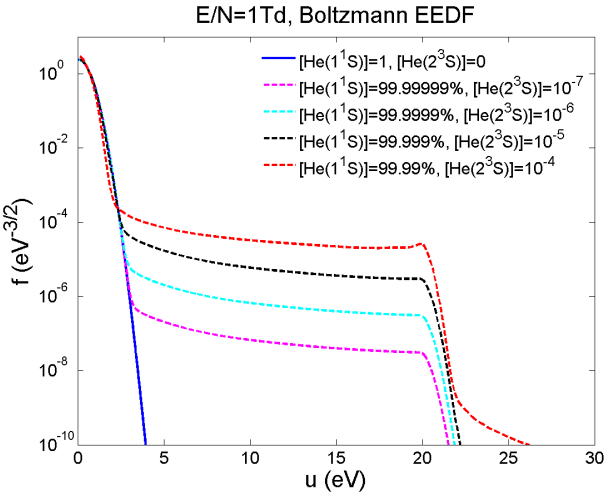

Figure 2. EEDF at $E/N = 1$ Td for several mixtures of helium ground-state and metastable He(2^3S).

At the range of the dozens of E/N, the EEDF seems to have a less energetic body but a more energetic tail when the metastable states are added. At values of E/N like 10 Td and 50 Td, comparatively to the case of 1 Td, inelastic collisions that require an energy threshold happen more often and superelastic collisions that have no requirement of electron energy lose importance.

We must take into consideration that ionization is obtained for electron energies higher than 3.97 eV for collisions with He(2^1S), 4.77 eV for collisions with He(2^3S) and 24.59 eV for collisions with ground-state He. Therefore, the addition of metastable relative densities of 10^{-7} - 10^{-4}, as the ones of figure 2 has a noticeable effect also in the calculated electron rate coefficients, particularly in the ionization coefficient, especially at low E/N. Figure 3 shows this effect for several mixtures of He(1^1S) and He(2^3S) over a range of E/N between 0.1 Td and 300 Td, where an evident influence of stepwise ionization reactions is perceived for reduced fields below 20 Td.

We notice in fig. 3 that even at the lowest fields, below 1 Td, stepwise ionization always exists, since it requires very low energy thresholds (4.77 eV and 3.97 eV). Therefore, the weighted ionization coefficient is higher the more we account for excited-state densities and for stepwise ionization. The effect of the stepwise ionization rates on the global ionization had already been reported in [5, 10]. For the low values of He(2^3S) concentrations expected, such as 10^{-6}, even though we can see the effect of stepwise ionization, its absolute value is low at $E/N < 2$ Td (K_{ion} at 1 Td $\sim 5 \times 10^{-24}$ m^3/s, while at 10 Td $\sim 10^{-19}$ m^3/s). However, for E/N between 2 Td and 20 Td, stepwise ionization appears to give a significant contribution to the global ionization coefficient. This is the direct consequence of the lower threshold ionization of metastables and of the plateaux in the EEDFs in fig. 2 that increase f_e at the ionization threshold energies, which is used to calculate K_{ion} through eq. (2).

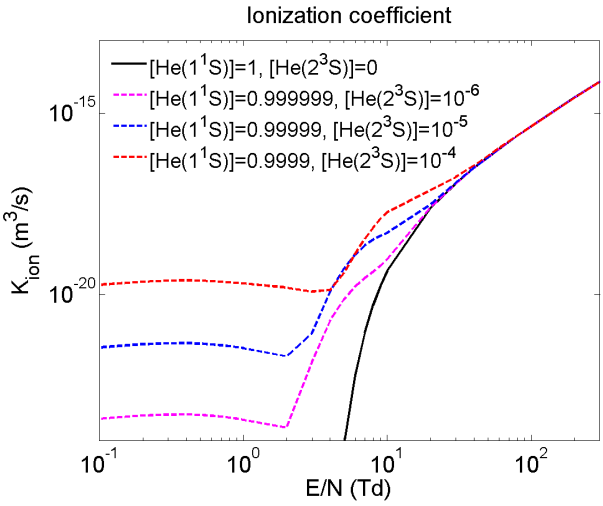

Figure 3. Electron-impact ionization coefficient in helium, as function of E/N, for different relative densities of He(1^1S) and He(2^3S).

2. *Solution for He-N_2-O_2 mixtures*

The addition of air constituents to He affects also the EEDF, as shown in figure 4 for He-N_2 mixtures (with He in ground-state) at $E/N = 10$ Td, where special attention is paid to scenarios at low N_2 densities. Note that this range of E/N – tens of Td – corresponds to the order of magnitude expected for the local reduced electric fields in atmospheric-pressure helium plasmas. In particular, 10 Td stays between the $\sim$ 5 Td reported in [6] for a steady-state discharge and the $\sim$ 40 Td reported in [11] for a propagation front in a tube. Results show that the atomic gas He presents a much more energetic EEDF than the molecular gas N_2. The excited and ionized states of He have very high energy thresholds, in contrast with the low-energy electronic and vibrational excited states of N_2, leading to a depletion of the EEDF tail when nitrogen is admixed. In fact, the introduction of N_2 and O_2 include

data for: elastic, rotational excitation, vibrational excitation (first energy threshold 0.29 eV), electronic excitation (6.17 eV) and ionization (15.5 eV) collisions between electrons and N_2; elastic, rotational excitation, vibrational excitation (0.19 eV), electronic excitation (0.98 eV), ionization (12.1 eV) and attachment collisions between electrons and O_2.

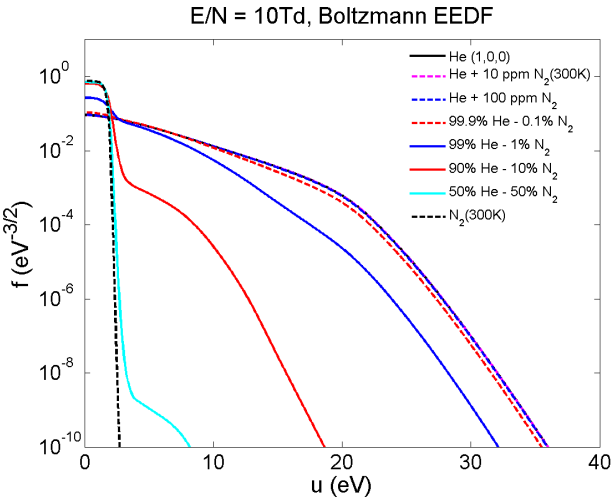

Figure 4. EEDF at E/N = 10 Td for several mixtures of He (ground-state only) and N_2.

In addition, we observe in figure 4 that even small admixtures of the molecular gases, like 1%, produce a significant change in the EEDF. The result is similar to the one reported in [12]. By increasing the amount of the molecular gas, we see that the EEDF of the mixture tends to approach the EEDF of the molecular gas at low energies, which means that the inelastic collisions with N_2 of low energy thresholds are dominating in this region. Although the EEDFs of N_2 and O_2 have different shapes due to the different excited states and energy thresholds, their effect on the EEDF when admixed with He with relative densities up to 1% is somewhat similar. As a result, so will be the effect of admixing synthesized air, composed of N_2 and O_2. At higher fields, like 50 Td, the effect of small admixtures is less noticeable. For example, it can not be remarked the depletion of the EEDF for an admixture of 0.1% of the molecular gas. On the contrary, at lower fields, such as 1 Td, there is a clearer difference in the shape of the EEDFs at low energies.

The changes observed in figure 4 for the EEDF induce differences also in the calculated rate coefficients, particularly in the global electron-impact ionization coefficient. Figure 5 presents the coefficient

$$K_{ion} = \frac{K_{He+}[He] + K_{N2+}[N_2]}{[He] + [N_2]}$$

for several He-N_2 mixtures, in the range of interest of E/N (1-100 Td). As predicted, the lower energy of the N_2 EEDF with respect to the He EEDF, leads to a much lower ionization coefficient in N_2 than He in the range of E/N considered. Results show that the admixture of small percentages of N_2 has little effect on the ionization coefficient, in coherence with the minor changes caused also in the EEDF (see figure 4). However, for the conditions of figure 5, a maximum of the ionization coefficient is obtained for an admixture of only 0.1% N_2 for fields lower than approximately 20 Td, while a large decrease is obtained already at 10% N_2 for the whole range of E/N.

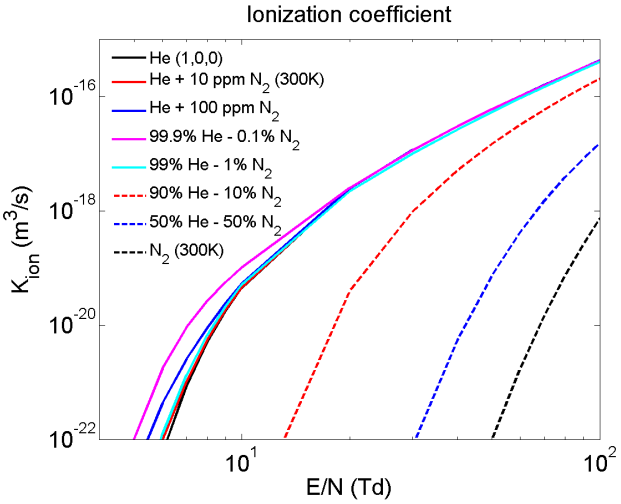

Figure 5. Ionization coefficient in helium, as function of E/N, for different relative densities of He(1^1S) and N_2.

In fact, the lower ionization threshold in N_2 than in He justifies that EEDFs similar to the one in pure He provide a higher ionization if only a small quantity of N_2 is added. This means that the coefficients for electron-He reactions (excitations and ionization) always decrease by the effect of the addition of N_2 but, on the contrary, the contribution of N_2 for direct ionization increases to a certain point until reaching a maximum, which depends on E/N. It then decreases thanks to the depletion of the EEDF, which explains the result obtained for the global coefficient. The overall result obtained for He-N_2 mixtures suggests that a small admixture of the molecular gas to He may be a helpful feature in order to create and maintain a discharge.

The effect in the EEDF of an admixture of O_2 is similar to the one observed for He-N_2 mixtures. However, the electronegativity of O_2 is shown to have an important effect on the plasma behavior. The inclusion of oxygen brings about the introduction of an electronic attachment process, $e^- + O_2 \rightarrow O^- + O$, which is why it is useful to use the EBE solver to calculate an effective ionization coefficient, defined as the difference between the electron-impact ionization and attachment coefficients. Figure 6 depicts the effect of that subtraction by comparing the effective coefficient in the range of E/N 1-100 Td for several mixtures of He with dry air (80%N_2-20%O_2), considering, therefore,

He ionization, N_2 ionization, O_2 ionization and O_2 attachment, with focus in small concentrations of air.

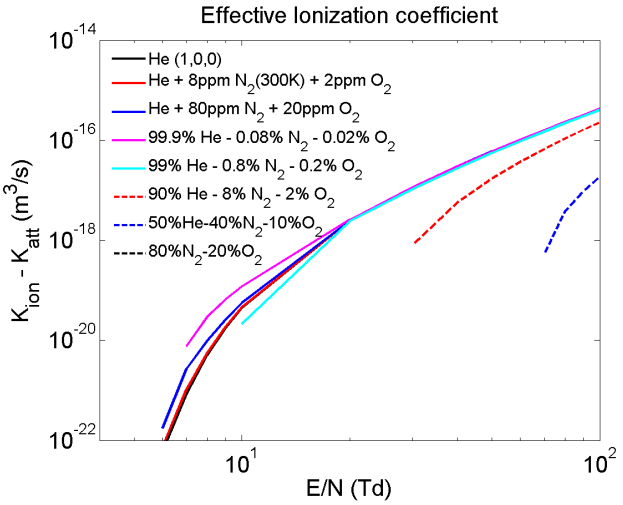

Figure 6. Effective ionization coefficient, as function of E/N, for different relative densities of He(1^1S) and dry air.

A major difference between the results presented in figures 5 and 6 is that the addition of O_2 (hence of an attachment mechanism) is responsible for the appearance of negative values in the effective ionization coefficient. These negative values are obtained at low reduced electric fields depending on the mixture composition (see the interrupted curves in figure 6), and they suggest enhanced difficulties in the breakdown of oxygen-containing plasmas.

In figure 7, we approach the analysis of He-air mixtures, this time noticing the evolution of the global ionization coefficient with air concentration for three relevant values of E/N, despising attachment. 5 Td is a value of reference, close to the E/N obtained in [6] at steady-state, and the other two chosen values of E/N, 20 Td and 60 Td, are intermediate fields in the range useful to study plasma propagation in tubes at atmospheric-pressure. The result is similar to those for He-N_2 mixtures and He-O_2 mixtures, with maxima of K_{ion} near 0.1% at 5 Td and near 1% at 20 Td. The N_2 and O_2 direct ionization increase with small amounts of air, as well as their excitation coefficients.

In the case of He-air mixtures without He metastables, equation 3 for the power balance includes all the power terms P_E, P_{sup}, P_{el}, P_{exc} and P_{ion}, including the power gained by the electrons from superelastic collisions, due to the N_2 vibrational states. It means that all the energy gained by the electrons through the effect of the electric field and superelastic collisions is spent in elastic and inelastic collisions and, in the latter case, can create an excitation or an ionization. Therefore, for each calculated EEDF, and thus for each input values of mixture and reduced electric field, a different amount of power is gained by electrons and the energy losses will undergo a different distribution between the possible processes.

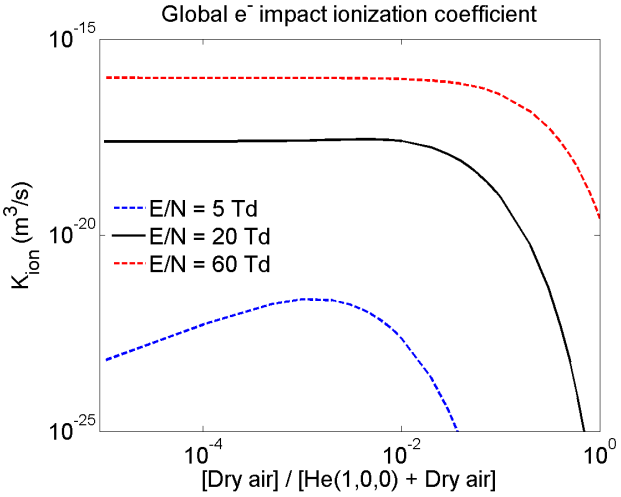

Figure 7. Global electron-impact ionization coefficients, as function of the relative density of dry air (80%N_2-20%O_2), for three values of E/N: 5 Td, 20 Td and 60 Td.

B. Pure He steady-state heavy species kinetics

The study of electron reactions alone, although important, is insufficient to provide a detailed description of the plasma, revealing its dominant species and their creation and loss mechanisms. For this purpose, reactions between heavy species have to be considered also, which demands solving the global system of rate balance equations for the different plasma constituents. In order to develop collisional-radiative models (CRMs) for He-based plasmas, that can subsequently be implemented in fluid models, IST-LoKI needs to be developed to include a CRM for He alone. The study of the discharge kinetics requires the solution of the rate balance equations,

$$\frac{\partial n_s}{\partial t} + \nabla.(n_s \vec{v_s}) = S_s - L_s \qquad (5)$$

coupled with the electron Boltzmann equation (1). IST-LoKI works with imposed pressure p, gas temperature T_g, oscillation frequency f, tube radius R, electron density n_e and gas mixture with the corresponding electron-impact cross sections. The homogeneous steady-state EBE for the EEDF is solved and the plasma transport parameters and electron-impact rate coefficients are calculated, as described in the previous section.

Then, the set of rate balance equations, for the different neutral and ion species, is solved using a Runge-Kutta method for ordinary differential equations. The reduced electric field E/N necessary to maintain the steady-state discharge is self-consistently determined as an eigenvalue solution to the problem. The charged particle net production rate must exactly compensate for the net loss rate, so as to satisfy the electron ionization-loss balance equation. In order to do so, E/N is iteratively calculated. Since the discharge provokes changes in the gas mixture composition,

depending on each E/N, the mixture for which the EEDF is calculated also requires self-consistency, under the demand that the EBE is solved for the final E/N and gas mixture calculated by the chemistry solver. Finally, the rate balance equations are solved for the same E/N and EEDF for the whole temporal evolution until reaching the steady-state condition.

By considering only the application of a steady-state electric field and the chemical and diffusion processes, we are isolating a part of the physics in the plasma from the global picture. However, by introducing a kinetic scheme for He, the zero-D simulations of IST-LoKI allow to understand the kinetics in the plasma in given conditions. A detailed kinetic scheme for a pure He P_{atm} discharge is given in [6], accounting for He^+, He_2^+, $He(n^{2s+1}l)$ and He_2^*, and providing indication on the most important species and reactions. In the present work, the definition of a collisional-radiative model using a reduced kinetic scheme for He heavy species is put forward using IST-LoKI, considering the conditions of interest for He plasma jets, which can serve as a first step for further study of He-based P_{atm} plasmas.

By respect to the scheme in [6], the scheme used in IST-LoKI does not contain the excited atomic states $He(n > 2, l, s)$, along with the associated reactions, among which the associative ionization $He(n > 2, l, s) + He \rightarrow He_2^+ + e^-$. Comparing the results obtained in the same plasma conditions with different reaction schemes, the scheme used in IST-LoKI is validated for given conditions but it is concluded that even a reduced scheme should include the excited species $He(n > 2)$ and the associative ionization reactions. Therefore, the comparison has given an indication for the future development of the He CRM using IST-LoKI.

The study of Helium-based collisional-radiative models intends to get us closer to study the plasma in the conditions of the jets presented in [11]. Therefore, after having validated a Helium reduced CRM, the tool IST-LoKI is used to study a plasma still in steady-state with a permanently applied electric-field but in closer conditions to our goal. As in [11], the gas temperature is set to the environment temperature $T_g = 300$ K, the pressure remains atmospheric $p = 101\,325$ Pa and the tube radius is set equal to the one used in the experiments in GREMI, $R = 2$ mm [4]. The field is taken as DC, with $f = 0$ and the imposed electron density is varied to cover the range obtained in [4, 11], between 10^9 and 10^{14} cm^{-3}.

The values of E/N calculated for the input electron densities are in the range 4-7 Td and increase with n_e. The results obtained show that for every value of electron density, He_2^+ is the dominant ion and the quasi-neutrality condition is obtained with $n_e \simeq [He_2^+]$. In figure 8 we observe the results for the densities of every He excited species in the plasma, variable with n_e and, therefore, with E/N. We infer that the excited species densities also increase with n_e and E/N, which is primarily due to the electron-impact reaction rates that increase directly with n_e and whose coefficients also increase with E/N, due to the more energetic EEDF. The relation between the excited species densities is variable with n_e and the metastable $He(2^3S)$, the radiative state $He(2^3P)$ and the excimer He_2^* have important densities, overcoming n_e in some occasions. $He(2^1P)$ always presents rather low densities and a more reduced scheme can consider its removal. The relative densities of the metastables $He(2^3S)$ and $He(2^1S)$ are variable between $\sim 10^{-9}$ when $n_e = 10^9$ cm^{-3} and $\sim 10^{-6}$ if $n_e = 10^{14}$ cm^{-3}, which is why, according to the results in figure 3, they can have some influence on the EEDF and on the excitation and ionization coefficients. The explanation for the species densities will be approached by studying the reactions responsible for each species balance.

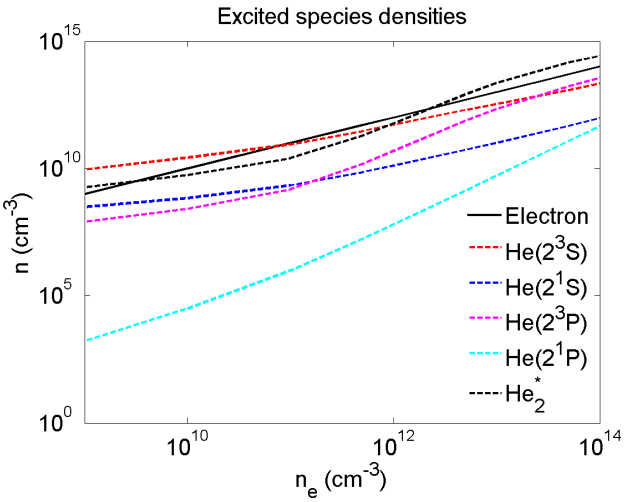

Figure 8. Atomic and molecular He excited species densities, along with the electron densities, as function of n_e.

The synthesis of the analysis made for He_2^+ and He^+ can be found in figures 9 and 10, where the set of reactions having influence on charge balance is represented, with the reactions assembled by groups. The numbers of reactions refer to the complete set of reactions, presented in the thesis. From figure 9, we take the conclusion that Penning ionization (R30-49) and stepwise ionization (R20-21) rates are always very important for charge creation in the discharge, reinforcing the role of the internal energy contained in the He excited states, transfered to ionization. In particular, the Penning reactions that depend on $He(2^3S)$ or $He(2^3P)$ are very important, while those depending on $He(2^1P)$ have irrelevant rates. Excimer ionization (R26) proves to be relevant at high n_e. As far as the destruction of electrons is concerned (see figure 10), dissociative recombination (R22-25) is essential at high n_e and diffusion of electrons/ions (R62-63) is important for charge loss at low n_e, while the electron-stabilized recombination rates (R27-29) are negligible.

Even though it does not influence charge balance directly, the charge transfer reaction $He^+ + 2\,He \rightarrow He_2^+ + He$

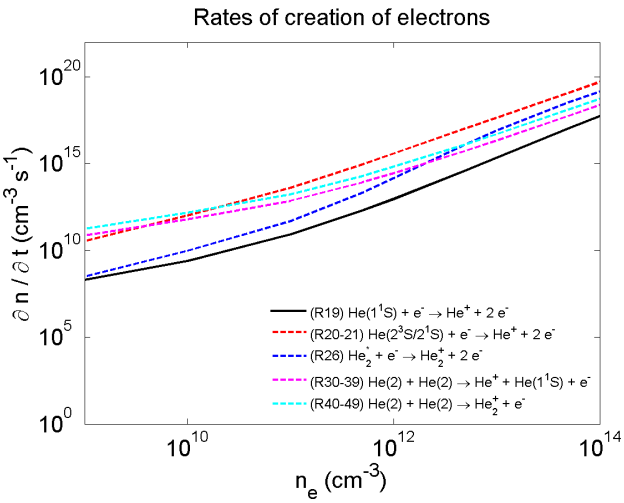

Figure 9. Rates of creation of electrons, discriminated by reaction, as function of n_e.

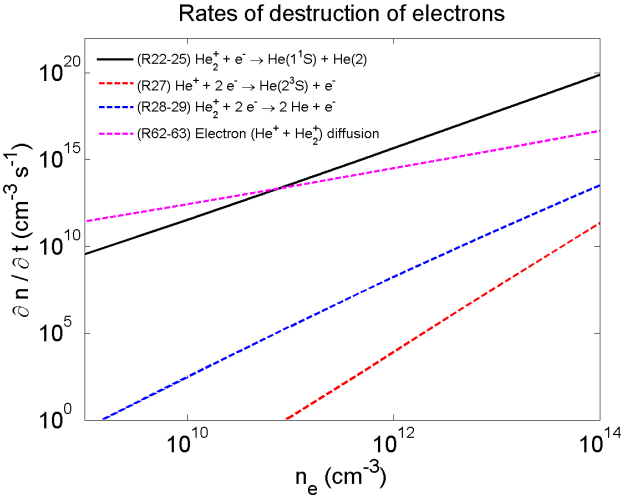

Figure 10. Rates of destruction of electrons, discriminated by reaction, as function of n_e .

has proved to be essential for the balance between the ion densities. On the contrary, the opposite charge transfer $He_2^+ \rightarrow He^+$ presents a rate ~ 30 orders of magnitude lower, due to the low T_g, on which the reaction rate coefficient depends. The fact that charge transfers only happen in one sense is the main factor to explain the difference of 2 to 5 orders of magnitude of the ion species densities.

Regarding the atomic He excited species, electron-impact excitation, stepwise excitation, de-excitation and stepwise ionization reactions, along with radiative transitions, are essential as the primary means of excitation of He and for the equilibrium between the excited states. As far as $He(2^3S)$ and $He(2^3P)$ are concerned, the association reactions, $He(2^3S/2^3P) + 2\ He \rightarrow He_2^* + He$, assume an important role in their destruction. The molecular excimer He_2^*, particularly relevant for ionization at high n_e, is created by these reactions and destroyed by the dissociation mechanisms $He_2^* + He \rightarrow He(2^3P) + 2\ He$.

Thinking of obtaining a more reduced scheme, we have learned that the species $He(2^1P)$ has a negligible role and can be dismissed, along with its reactions, including Penning ionization. The electron-stabilized recombination reactions can also be discarded due to their despicable influence. The charge transfer rate from He_2^+ towards He^+ has proved to be highly sensitive to T_g and, if the model imposes $T_g = 300$ K, this reaction can be excluded. The extrapolation of these conclusions to a case using a more complete scheme with $He(n > 2, l, s)$ species or to the case of a jet with a pulsed electric field has to be done carefully.

C. He-N_2 kinetics in a tube streamer

Following the previous chapters where we have studied the electron kinetics and related parameters in He-based mixtures and the kinetics of a plasma with Helium gas alone at steady-state, we now want to move forward to the study of a He plasma with impurities of the air gases N_2 and O_2. At the EM2C laboratory, we have studied the zero-dimensional kinetics of a He-N_2 plasma, simulating the conditions of an ionization wave in a tube at atmospheric-pressure and room-temperature, as in [11]. Understanding the influence of small concentrations of N_2 on the characteristics of a He-based discharge propagating along a dielectric tube is set as the objective, which requires coupling zero-D results for kinetics alone with 2D results of discharge dynamics in the tube, developed at the EM2C.

At present, the task of studying the zero-D estimation of the ionization wave plasma in the tube is done using tools other than IST-LoKI. An on-line free-ware zero-dimensional plasma kinetics solver was used to study the temporal evolution of He-N_2 discharges. ZDPlasKin [13] is a module designed to follow the time evolution of the species densities and the temperatures in a non-thermal plasma with an arbitrary chemistry. Unlike IST-LoKI, used in the previous sections, here the applied reduced electric field at each time can be imposed. All the species densities are calculated as function of this field at each time, including the electron density. In this work, the choice for the electric field is an estimation of the field in the discharge front from 2D simulations, as the ones in [11]. It has been used a peak with a minimum of 0.4 Td and a maximum of 50 Td, centered around 10 ns, with a rise time of 8 ns and a $width = 0.2$ ns.

The region of time studied is a simulation of the discharge front and the time posterior to the field application, which we call post-discharge, simulates what happens in the channel after the passage of the ionization front. In the figures presented from here forward, such as figure 11, the electric field is represented on the right-side inverted vertical-axis. Pre-ionization is defined as 10^9 cm^{-3} for e^- and N_2^+, the species that stay longer in post-discharge. For each instant

in time, ZDPlasKin [13] finds the user-defined local electric field and automatically calls the electron Boltzmann equation solver Bolsig+ [5], that provides a rapid calculation of electron transport parameters and rate coefficients. The rate equations (5) for the species densities are integrated in time.

In [14], a kinetic scheme has been derived from the detailed experimental study of an atmospheric-pressure discharge in helium with small admixtures of N_2. In this kinetic scheme, the importance of three-body reactions, Penning ionization, ion conversion and charge transfer was evidenced. It intends to represent a reduced scheme of He-N_2 reactions for low reduced fields, $E/N < 80$ Td. In the present work, that kinetic scheme is reduced by taking into account 4 positive ions (He^+, He_2^+, N_2^+, $N_2^+(B)$), the metastable $He(2^3S)$, the radiative $N_2(C^3\Pi_u)$ and electrons.

Here, the influence of nitrogen admixtures on the discharge kinetics is studied. Figure 11 shows the temporal evolution of the electron density behind the discharge front of a typical atmospheric-pressure discharge, propagating in a tube as in [11], for three different amounts of N_2 added to He: 10, 1000 and 30 000 ppm. Calculations use as input the time evolution values of the local transitory electric field, also presented in figure 11.

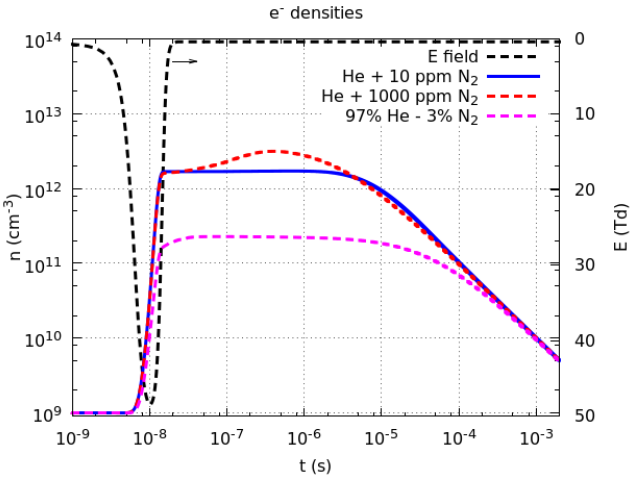

Figure 11. Temporal evolution of the local electron density, for local transitory pulsed field with 50 Td maximum amplitude.

Figure 11 shows that the admixture of low concentrations of N_2 (1000 ppm) leads to an increase in the electron density of the post-discharge behind the discharge front. These results are coherent with those of figure 5, where the highest ionization coefficient is attained at the order of 1000 ppm of N_2. However, higher concentrations of N_2 (e.g. 3%) lead to much lower ionization levels due to the decrease in the initial electron-impact ionization coefficient, in accordance with the results shown in figures 4 and 5. In the particular case of atmospheric-pressure plasma propagation in tubes, the ionization level behind the discharge front affects the conductivity of the plasma in the tube, hence the discharge dynamics and structure. The kinetic effects will therefore influence the jet propagation length and velocity. The discharge propagation is faster and larger for N_2 concentrations in the order of 1000 ppm. In fact, there is a big increase of dynamics between the small concentrations of N_2 of 10 or 100 ppm and 1000 ppm and there is a small decrease between 0.1% and 1% of N_2 in the mixture. These results agree qualitatively with those obtained experimentally in [4], where there is a change in velocity with a maximum for 2500 ppm of N_2 and a change of the discharge structure with the variation of the N_2 concentration.

For the particular case of 1000 ppm of N_2, the influence of some species and reactions is studied with more detail. In particular, the importance of Penning reactions ($He(2^3S) + N_2 \rightarrow He + N_2^+ + e^-$) on the discharge structure is quantified. Figures 12 and 13 compare the plasma composition when Penning reactions are included and discarded. They allow to notice that both He ion densities, $[He^+]$ and $[He_2^+]$, rise during the ionization front and decrease quickly to 10^8 cm^{-3} in about 100 ns and 130 ns, respectively. $[He(2^3S)]$ also rises during the electric field application but stays longer in post-discharge. N_2^+ density, which increases both during the electric field application and in post-discharge is clearly the dominant ion starting from 40 ns into post-discharge.

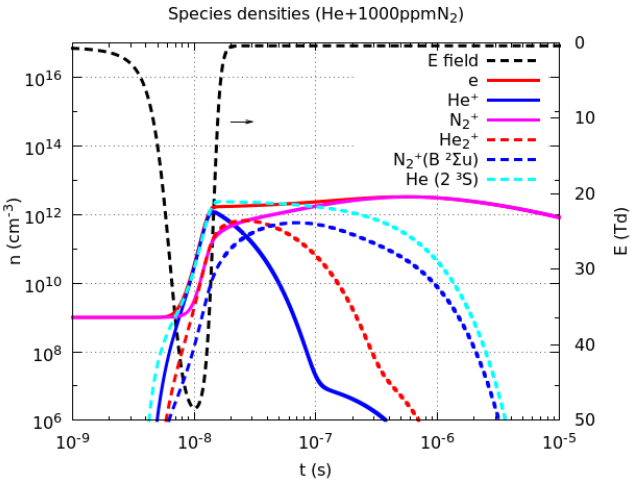

Figure 12. Temporal evolution of the local density of species, for local transitory pulsed field with 50 Td maximum amplitude. Simulation results considering the full kinetic scheme.

These figures also reveal that Penning reactions crucially change the ionization level in the post-discharge behind the discharge front, showing the importance of both $He(2^3S)$ and N_2 species on the discharge dynamics and further explaining the relevance of N_2 admixture. In fact, due to Penning ionization, electron creation in the early post-discharge is significantly higher near 1000 or 10 000 ppm of N_2 than for lower concentrations, thanks to N_2 density. Therefore, the dynamics of propagation depends greatly on Penning ionization in early post-discharge, before 10 μs af-

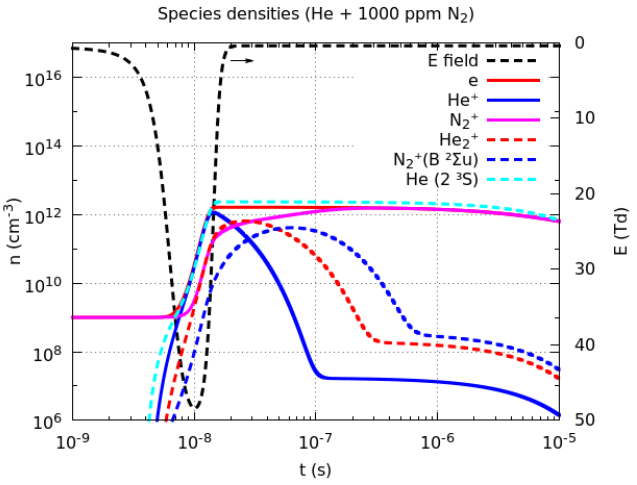

Figure 13. Temporal evolution of the local density of species, for local transitory pulsed field with 50 Td maximum amplitude. Simulation results discarding Penning reactions from the kinetic scheme.

ter the field passage.

III. CONCLUSIONS

The importance of electron-impact reactions in helium-based plasmas has been analyzed with numerical simulations, using either the IST-LoKI tool or the ZDPlasKin and Bolsig+ solvers. The influence on the EEDF of the He metastable states causing superelastic collisions was documented. Metastable states were proven to affect also the global electron-impact ionization in the discharge, depending of their densities, due to stepwise ionization reactions.

EEDFs have been compared for different mixtures of He with the atmospheric gases N_2 and O_2, exhibiting higher tails in the pure noble gas. The effect of these mixtures on the calculated electron-impact rate coefficients has also been registered, with emphasis on the global ionization coefficient. The cases of low molecular gas densities, around 0.1%, were shown to provide higher ionization coefficients than the case of pure He, due to the low ionization thresholds of N_2 and O_2. The electronegativity of O_2 was shown to affect the electron kinetics, as a result of the electron attachment mechanism. The analysis of the effective ionization rate coefficient shows that discharge breakdown is more difficult in the presence of O_2.

A collisional-radiative model for pure He has been studied for steady-state conditions at atmospheric-pressure and room-temperature for different input electron densities. The relevance of species and reactions has been highlighted and a reduction for the studied scheme has been proposed, discarding the least relevant elements. The reduced CRM will serve as basis for reduced models for He-N_2-O_2 mixtures in given conditions.

Particle balance equations have been solved for a reduced He-N_2 kinetic scheme, considering the local application of a transitory electric field with 50 Td maximum amplitude at atmospheric-pressure and room-temperature, simulating the propagation of a jet ina tube in zero-dimensions. The key role of kinetic processes, especially Penning reactions, on the ionization degree of the plasma has been put forward. Moreover, the relation between nitrogen admixture and the different elementary processes participating in the kinetics has been studied and discussed, revealing the influence of N_2 on the plasma ionization level and its implications in the discharge structure.

IV. ACKNOWLEDGEMENTS

Work partially funded by Portuguese FCT – Fundação para a Ciência e Tecnologia, under Project UID/FIS/50010/2013.

[1] G. Y. Park et al., *Plasma Sources Sci. Technol.* 21, 043001 (2012)
[2] R. Rahul et al., *J. of Phys. D: Appl. Phys.* 38, 1750 (2005)
[3] E. Robert, E. Barbosa, S. Dozias, M. Vandamme, C. Cachoncinlle, R. Viladrosa and J-M. Pouvesle, *Plasma Process. Polym.* 6, 795 (2009)
[4] T. Darny, E. Robert, S. Dozias and J-M. Pouvesle, Proceedings of the conference *Gas Discharges* (2014)
[5] G. J. M. Hagelaar and L. C. Pitchford, *Plasma Sources Sci. Technol.* 14, 722-733 (2005)
[6] M. Santos, C. Noël, T. Belmonte and L. L. Alves, *J. Phys. D: Appl. Phys.* 47, 265201 (2014)
[7] G. Gousset, L. L. Alves and C. M. Ferreira, *J. Phys. D: Appl. Phys.* 25, 1713 (1992)
[8] S. Panchesnyi et al., The LXCat project, *30th International Conference on Phenomena in Ionized Gases* (ICPIG 2011)
[9] C. Gorse, M. Cacciatore, M. Capitelli, S. De Benedicts and G. Dilecce, *Chemical Physics* 119, 63 (1988)
[10] F. Paniccia, C. Gorse, J. Bretagne and M. Capitelli, *J. Appl. Phys.* 61, 8 (1987)
[11] J. Jansky and A. Bourdon, *Plasma Sources Sci. Technol.* 23, 025001 (2014)
[12] G. M. Petrov et al., *Plasma Chemistry and Plasma Processing* 20, 2 (2000)
[13] S. Pancheshnyi, B. Eismann, G. J. M. Hagelaar and L. C. Pitchford, Computer code ZDPlasKin, http://www.zdplaskin.laplace.univ-tlse.fr (2008)
[14] J-M. Pouvesle, A. Bouchoule and J. Stevefelt, *J. Chem. Phys.* 77, 817 (1982)